

EFFICIENT TEST-TIME PROMPT TUNING FOR VISION-LANGUAGE MODELS

Yuhan Zhu^{1,*} Guozhen Zhang¹ Chen Xu¹ Haocheng Shen² Xiaoxin Chen²
Gangshan Wu¹ Limin Wang^{1,3,†}

¹State Key Laboratory for Novel Software Technology, Nanjing University

²vivo AI Lab ³Shanghai AI Laboratory

zyuhan0812@gmail.com lmwang@nju.edu.cn

ABSTRACT

Vision-language models have showcased impressive zero-shot classification capabilities when equipped with suitable text prompts. Previous studies have shown the effectiveness of test-time prompt tuning; however, these methods typically require per-image prompt adaptation during inference, which incurs high computational budgets and limits scalability and practical deployment. To overcome this issue, we introduce Self-TPT, a novel framework leveraging Self-supervised learning for efficient Test-time Prompt Tuning. The key aspect of Self-TPT is that it turns to efficient predefined class adaptation via self-supervised learning, thus avoiding computation-heavy per-image adaptation at inference. Self-TPT begins by co-training the self-supervised and the classification task using source data, then applies the self-supervised task exclusively for test-time new class adaptation. Specifically, we propose Contrastive Prompt Learning (CPT) as the key task for self-supervision. CPT is designed to minimize the intra-class distances while enhancing inter-class distinguishability via contrastive learning. Furthermore, empirical evidence suggests that CPT could closely mimic back-propagated gradients of the classification task, offering a plausible explanation for its effectiveness. Motivated by this finding, we further introduce a gradient matching loss to explicitly enhance the gradient similarity. We evaluated Self-TPT across three challenging zero-shot benchmarks. The results consistently demonstrate that Self-TPT not only significantly reduces inference costs but also achieves state-of-the-art performance, effectively balancing the efficiency-efficacy trade-off.

1 INTRODUCTION

Open-set image classification is a fundamental yet challenging task in computer vision. Recently, Vision-Language Models (VLMs) (Jia et al., 2021; Li et al., 2022; Alayrac et al., 2022; Fang et al., 2023) have shown promising capabilities in this field. A prominent model, CLIP (Radford et al., 2021), encodes both images and language into a unified embedding space, allowing classification by measuring similarities between image representations and textual class descriptions.

Effective prompts for input classes are essential (Radford et al., 2021), but manually crafting them is time-consuming (Zhou et al., 2022b). Inspired by NLP advancements (Shin et al., 2020; Zhong et al., 2021), researchers have explored using continuous vectors as soft prompts, optimizing them with a few labeled data (source data). These methods can automatically obtain task-specific prompts, thereby improving performance (Zhou et al., 2022b; Zhu et al., 2024a). However, the source data is unlikely to encompass *all* possible classes, resulting in suboptimal *open-set* performance.

Test-time adaptation (TTA) (Liang et al., 2020a; Wang et al., 2020; Niu et al., 2023) has recently gained attention for adapting models to new data distributions during the test phase. In this context, TPT (Shu et al., 2022) was proposed to tune prompts for new classes at test time, thereby improving open-set generalization. As depicted in Fig. 1(a), TPT first learns prompts from source data (stage

*Work is done during internship at vivo AI Lab

†Corresponding author

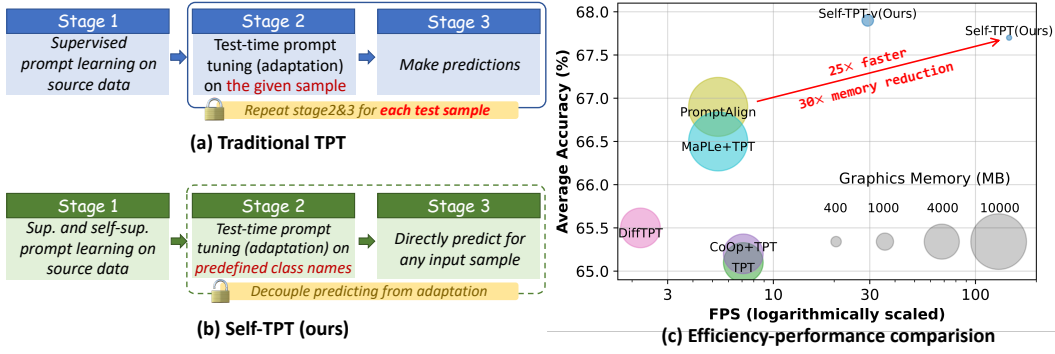


Figure 1: **TPT versus Self-TPT.** (a) TPT learns prompts from source data (stage 1), then adapts them to individual samples for prediction (stages 2&3). (b) Self-TPT employs text-oriented self-supervised learning (SSL) for joint training (stage 1) and for new class adaptation (stage 2), followed by *direct* predictions for each image (stage 3). (c) We present the frame per second (FPS) and graphics memory usage for each method when applied to CLIP-B/16 using the same A100-80G GPU. The y-axis represents the average cross-dataset accuracy.

1). It then adjusts these prompts for each test sample (stage 2) and uses the sample-tailored prompts for predictions (stage 3). Despite its effectiveness, TPT suffers from a significant computational budget during inference. *For each test sample*, it requires multiple forward and backward passes through the model and needs to retain the full computational graph, resulting in substantial latency and memory usage. As shown in Fig. 1(c), TPT operates at ~ 7 FPS while consuming ~ 5 GB of graphics memory. The latest TPT-based method, PromptAlign (Samadh et al., 2023), operates at ~ 5 FPS with ~ 11 GB of graphics memory. These heavy computational demands pose challenges for scaling TPT to larger VLMs and deploying it on resource-limited platforms, such as edge devices.

Can we leverage the generalization capability of TTA while minimizing the computational overhead? We observed that, during testing, while images are processed sequentially, the list of candidate class names is predetermined. Motivated by this, we introduce Self-TPT, an efficient Test-time Prompt Tuning framework that employs *text-oriented* Self-supervised learning (SSL). As depicted in Fig. 1(b), the adaptation process (stage 2) of Self-TPT operates solely on the predefined class names, allowing for *direct* predictions for any image without the need for prompt updates (stage 3), significantly reducing the computational load during inference.

For the SSL component, we follow the good practice in TTA (Chen et al., 2022a) to adopt contrastive learning. Effective classification requires that embeddings of the same class align relatively closely, while those from different classes remain distinct to ensure inter-class distinguishability. To achieve this, we introduce Contrastive Prompt Tuning (CPT). In CPT, we vary the insertion points of the class token within prompt sequences as data augmentation to create positive pairs. Negative pairs are built by contrasting a class against all others, thereby explicitly reinforcing the dissimilarity among class embeddings. Initially, we integrate CPT with supervised learning (stage 1) and subsequently rely exclusively on CPT for new class adaptation (stage 2).

Our empirical analysis reveals that CPT and classification tasks exhibit a consistently positive gradient correlation across 11 datasets. This correlation suggests that both tasks drive the model’s optimization in similar directions, allowing CPT to effectively act as a proxy for supervised learning during the adaptation phase. Inspired by this finding, we introduce a gradient matching (GM) loss specifically designed to enhance this positive correlation further. The GM loss operates on the gradients derived from both supervised and CPT losses and aims to maximize their cosine similarities.

We evaluated Self-TPT’s performance on three challenging benchmarks: cross-dataset generalization, base-to-new generalization, and domain generalization. Our findings reveal that Self-TPT consistently surpasses the prior state-of-the-art, PromptAlign, improving by 0.93%, 1.59%, and 1.82% on these benchmarks, respectively. Notably, Self-TPT significantly enhances efficiency, as shown in Fig. 1(c), achieving a 25-fold increase in inference speed and reducing memory usage by 30-fold compared to PromptAlign. Additionally, our tests also verify that Self-TPT is data-efficient and generalizes well across various model backbones, scales, and VLMs.

2 RELATED WORK

Vision-Language Models. Recent advances in computer vision and natural language processing have spurred significant interest in vision-language models (VLMs) (Radford et al., 2021; Jia et al., 2021; Li et al., 2022; Zhai et al., 2022; Alayrac et al., 2022; Fang et al., 2023). These models excel in various multi-modal tasks by leveraging massive datasets of image-text pairs to develop robust representations that span different modalities. Notably, CLIP (Radford et al., 2021) has demonstrated exceptional open-vocabulary capabilities, enabling effective performance in image classification (Zhou et al., 2022b; Zhu et al., 2024a), video recognition (Weng et al., 2023; Huang et al., 2024), and object detection (Du et al., 2022; Minderer et al., 2022), *etc.* A key aspect of deploying VLMs successfully involves crafting effective text prompts. In this paper, we introduce a novel framework that optimizes prompt adaptation for better class comprehension during testing.

Prompt Learning. Recent advancements in NLP have inspired approaches like CoOp (Zhou et al., 2022b; Chen et al., 2022b; Lu et al., 2022), which treats prompts for VLMs as continuous vectors. However, CoCoOp (Zhou et al., 2022a) highlighted a significant flaw: these learned prompts often overfit to seen classes, compromising performance on new ones. To mitigate this, recent studies have introduced additional learnable components (Zhu et al., 2024a; Zhou et al., 2022a; Khattak et al., 2023a; Zang et al., 2022; Wang et al., 2023c; Singha et al., 2023) or specialized strategies (Lee et al., 2023; Xu et al., 2023b; Long et al., 2023; Shi & Yang, 2023; Kan et al., 2023; Wang et al., 2023a) to enhance prompt generalization. Techniques like distillation and regularization (Yao et al., 2023; Zhu et al., 2022; Khattak et al., 2023b; Xu et al., 2023a; Bulat & Tzimiropoulos, 2023) are also employed to integrate task-specific knowledge and hand-crafted priors. Despite progress, achieving prompts that generalize across all possible classes remains challenging. Consequently, this paper shifts focus to test-time adaptation strategies, dynamically adjusting prompts during testing to address open-world application challenges.

Test-Time Adaptation was developed to address shifts in data distribution between training and testing phases by dynamically adjusting the model to the test sample. Numerous methods have emerged, including entropy minimization (Liang et al., 2020a; Wang et al., 2020; Niu et al., 2023), activation of batch-normalization statistics (Wang et al., 2020; Zhao et al., 2023; Niu et al., 2023), pseudo labeling (Chen et al., 2022a; Liang et al., 2020b; Wang & Wibisono, 2022), feature alignment (Liu et al., 2021; Wang et al., 2023b; Wang & Aitchison, 2022), and test-time training (Sun et al., 2020; Liu et al., 2021; Huang et al., 2021; Chen et al., 2023; Gandselman et al., 2022). Recently, test-time prompt tuning (TPT) (Shu et al., 2022) for VLMs has gained attention. TPT optimizes prompts by reducing prediction entropy and uses image augmentation to create prediction diversity. Techniques like DiffTPT (Feng et al., 2023) employ Stable Diffusion (Rombach et al., 2022) to boost augmented image diversity, while SwapPrompt (Ma et al., 2023) and PromptAlign (Samadh et al., 2023) focus on maximizing prediction agreement and aligning token statistics, respectively. Despite their effectiveness, these approaches often entail high computational costs during inference, posing challenges for practical deployment. This study introduces a more efficient framework for test-time prompt tuning, aiming to balance effectiveness with real-world applicability.

3 METHOD

3.1 PRELIMINARIES

Contrastive Language-Image Pre-training (CLIP) (Radford et al., 2021) encodes image x and a set of class descriptions $\{t_i\}_{i=1}^C$ into a joint vision-language embedding space using two encoders: the image encoder $f(\cdot)$ and the text encoder $g(\cdot)$. Here, C denotes the number of candidate classes. This embedding space ensures inputs sharing similar concepts are closely aligned. In this way, the classification problem can be formulated as an image-text matching problem. Specifically, CLIP computes the encoded image feature e and the encoded text features $\{w_i\}_{i=1}^C$. The probability for the i -th class is calculated as:

$$p(y_i | x) = \frac{\exp(\cos(w_i, e) / \tau)}{\sum_{j=1}^C \exp(\cos(w_j, e) / \tau)}, \quad (1)$$

where τ is a temperature parameter.

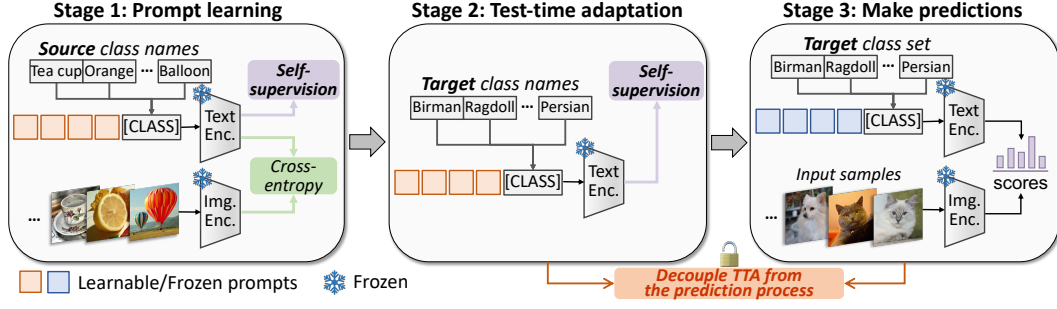


Figure 2: **Overview of Self-TPT.** Self-TPT operates in three stages. Stage 1: Conduct prompt learning on a source dataset, co-trained with a self-supervised loss. Stage 2: Perform test-time adaptation (TTA) for new class understanding via the self-supervised loss. Stage 3: Perform direct predictions on the target dataset without further adjustment of the prompts.

Prompt Learning (Zhou et al., 2022b;a; Yao et al., 2023; Zhu et al., 2022) aims to optimize soft prompts $\mathbf{P} \in \mathbb{R}^{M \times d}$ to replace manually designed prompts (e.g., “a photo of a [CLASS]”):

$$\mathbf{t}_i = [P]_1[P]_2 \dots [P]_M[\text{CLASS}]_i, \quad i = 1, \dots, C \quad (2)$$

Here, $[\text{CLASS}]_i$ are the word embeddings for the i -th class and d is the dimension of the word embeddings used in CLIP. The parameters of \mathbf{P} , represented as θ_p , are shared across all classes. The training dataset (i.e., source data), denoted as $\mathcal{S} = (\mathcal{X}^{(s)}, \mathcal{Y}^{(s)}, \mathcal{M}^{(s)})$, includes images $\mathcal{X}^{(s)}$, candidate class names $\mathcal{Y}^{(s)}$, and a ground-truth mapping $\mathcal{M}^{(s)}$ between them. Training employs a cross-entropy loss function:

$$\min_{\theta_p} \mathcal{L}_{ce} \left(\mathcal{X}^{(s)}, \mathcal{Y}^{(s)}, \mathcal{M}^{(s)}; \mathbf{P}, f, g \right). \quad (3)$$

During this training phase, the image and text encoders from CLIP are kept frozen.

Test-time Prompt Tuning (TPT) (Shu et al., 2022; Feng et al., 2023; Samadh et al., 2023) aims to dynamically adapt prompts to unlabeled test data $\mathcal{T} = (\mathcal{X}^{(t)}, \mathcal{Y}^{(t)})$, where $\mathcal{X}^{(t)}, \mathcal{Y}^{(t)}$ represent the target images and candidate class names, respectively. TPT involves three stages: Initially, training prompts on source data. Then, using the prompts from first stage, TPT employs an unsupervised loss, such as entropy minimization \mathcal{L}_{ent} , to tailor these prompts for each specific test sample $\mathcal{X}_i^{(t)}$:

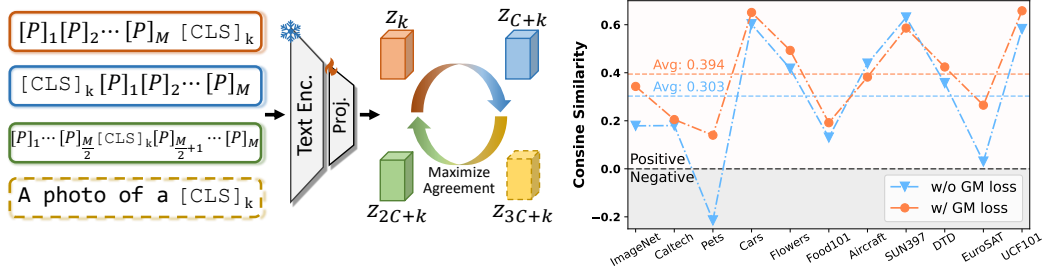
$$\min_{\theta_p} \mathcal{L}_{ent} \left(\mathcal{X}_i^{(t)}, \mathcal{Y}^{(t)}; \mathbf{P}, f, g \right). \quad (4)$$

Subsequently, predictions are made for each sample using these tailored prompts. Despite their effectiveness, these methods are computationally intensive during inference. Each test sample requires multiple model passes and retention of a full computational graph, leading to increased latency and significant memory demands. These limitations make deployment challenging, particularly in resource-constrained environments like edge devices, and hinder scalability to larger VLMs.

3.2 PIPELINE OF SELF-TPT

To leverage the generalization ability of test-time adaptation while minimizing computational overhead during inference, we propose Self-TPT, an efficient Test-time Prompt Tuning method based on Self-supervised learning. Given the source data \mathcal{S} and target data \mathcal{T} with a potentially disjoint class set, our objective is to obtain prompts for VLMs to well-classify the images in \mathcal{T} . Self-TPT acquires task-specific knowledge from the source data and adapts these learned prompts to new classes at test time, without directly assessing the specific images from \mathcal{T} . The overall pipeline of Self-TPT, as depicted in Fig. 2, comprises three stages: prompt learning, test-time adaptation, and direct prediction. In Stage 1, we co-train the self-supervised task and the classification task:

$$\min_{\theta_p, \theta_h} \mathcal{L}_{ce} \left(\mathcal{X}^{(s)}, \mathcal{Y}^{(s)}, \mathcal{M}^{(s)}; \mathbf{P}, f, g \right) + \mathcal{L}_{ssl} \left(\mathcal{Y}^{(s)}; \mathbf{P}, g, h \right), \quad (5)$$



(a) **Contrastive Prompt Tuning.** Class token “[CLS]” is inserted at the front, end, and middle in the prompt sequences to generate positive pairs for contrastive learning. An additional hand-made prompt is incorporated as regularization. (b) **Cosine similarity** between CPT and the classification task gradients across 11 datasets. A positive correlation can be observed between the two tasks. This correlation can be further enhanced by the gradient matching (GM) loss.

Figure 3: **Contrastive Prompt Tuning and Gradient Similarity Analysis.**

where $h(\cdot)$ is a SSL projection head, and θ_h denotes its parameters. In Stage 2, given the class set $\mathcal{Y}^{(t)}$ of \mathcal{T} , we adapt using a text-oriented SSL task, decoupling the test-time adaptation from specific test samples $\mathcal{X}_i^{(t)}$:

$$\min_{\theta_p} \mathcal{L}_{ssl}(\mathcal{Y}^{(t)}; \mathbf{P}, g, h). \quad (6)$$

The prompts refined through Eq. 6 are directly applied to predict samples in \mathcal{T} without further adjustments, thereby streamlining the test-time adaptation into a pre-processing step and significantly reducing computational costs during inference. In Sec. 3.3, we will detail the specific SSL tasks used in our Self-TPT framework, and in Sec. 3.4, we will empirically demonstrate how our SSL tasks facilitate improved classification performance.

3.3 CONTRASTIVE PROMPT TUNING

Within the Self-TPT framework, the core design is its self-supervised component. As indicated by Sun et al. (2020), the auxiliary task (in this case, the SSL task) should have a strong correlation with the main task (in this case, the classification task) to maintain effectiveness. In the realm of self-supervised learning, contrastive learning methods (Chen et al., 2020; He et al., 2020) have yielded impressive classification outcomes, even through the linear probing of frozen visual representations. This underscores a positive connection between contrastive tasks and classification tasks, thereby motivating our prioritization of contrastive learning in the SSL task design.

To construct the contrastive task, we adhere to the nature of classification that embeddings from the same class should align closely, while those from different classes should remain distinct to ensure inter-class distinguishability. To this end, we introduce a novel task named Contrastive Prompt Tuning (CPT). This task varies the insertion points of the class token “[CLS]” within prompt sequences to generate positive pairs. As depicted in Fig. 3a, CPT strategically places the “[CLS]” token at the beginning, end, and middle of the learnable prompts:

$$\begin{aligned} t_k &= [P]_1[P]_2 \dots [P]_M[CLS]_k, \\ t_{C+k} &= [CLS]_k[P]_1[P]_2 \dots [P]_M, \\ t_{2C+k} &= [P]_1 \dots [P]_{\frac{M}{2}}[CLS]_k[P]_{\frac{M}{2}+1} \dots [P]_M. \end{aligned} \quad k = 1, \dots, C \quad (7)$$

Furthermore, Zhu et al. (2022) suggests that a simple, hand-crafted prompt (e.g., “a photo of a”) embodies the general knowledge acquired during pre-training and can mitigate overfitting. With this insight, we incorporate such prompt into CPT to regulate the contrastive learning process:

$$t_{3C+k} = [a][photo][of][a][CLS]_k. \quad k = 1, \dots, C \quad (8)$$

Eq. 7 and Eq. 8 establish four distinct views for each class. Let $i \in \{1, \dots, 4C\}$ denote the index of a specific view from any class. We define the index set of its three other views as $\mathcal{P}_{(i)} \equiv \{i \bmod$

Table 1: **Comparing inference computational costs.** “FPS” denotes frames per second. All tests are conducted on the same single A100 GPU and performed on ImageNet with a batch size of 1. Self-TPT-v is introduced in Implementation Details.

Method	Venue	CLIP-B/16		CLIP-L/14	
		FPS (↑)	Memory (↓)	FPS (↑)	Memory (↓)
TPT (Shu et al., 2022)	NeurIPS’22	7.1	5.2GB	3.3	8.5GB
DiffTPT (Feng et al., 2023)	ICCV’23	2.2	5.2GB	1.0	8.5GB
PromptAlign (Samadh et al., 2023)	NeurIPS’23	5.3	11.2GB	2.1	31.5GB
Self-TPT	–	146.7	0.32GB	81.6	0.86GB
Self-TPT-v	–	29.3	0.66GB	7.9	1.41GB

$C, i \bmod C + C, i \bmod C + 2C, i \bmod C + 3C\} \setminus \{i\}$. The CPT loss is then formulated as:

$$\mathcal{L}_{CPT} = - \sum_{i=1}^{4C} \log \frac{\sum_{j \in \mathcal{P}_{(i)}} \exp(z_i \cdot z_j / \tau)}{\sum_{j=1, j \neq i}^{4C} \exp(z_i \cdot z_j / \tau)}. \quad (9)$$

Here, z denotes the text feature after projection, computed as $z_i = h(g(t_i))$, and τ is a scaling temperature parameter, defaulting to 0.07.

3.4 GRADIENT MATCHING

A pertinent question arises: how does CPT benefit classification during adaptation? To uncover the underlying reasons, we conducted an empirical analysis by measuring the cosine similarity of gradients between the classification loss and the CPT loss during optimization, expressed as:

$$\cos(\nabla_{\mathcal{L}_{ce}}, \nabla_{\mathcal{L}_{CPT}}), \quad (10)$$

where ∇ denotes the gradients corresponding to each loss. $\nabla_{\mathcal{L}_{ce}}$ is computed as the average over all images in the dataset to ensure statistical significance. The resulting similarity scores, depicted as blue triangles in Fig. 3b, show positive correlations in 10 out of the 11 datasets examined. The direction of these gradients suggests that CPT can effectively align with the optimization pathways of the classification task during test-time adaptation, even in the absence of ground-truth labels.

Inspired by this finding, we propose a Gradient Matching (GM) loss to explicitly improve gradient similarity between the two tasks. During training, we noted that $\nabla_{\mathcal{L}_{ce}}$ exhibits sensitivity to small batch sizes. To obtain the stable optimization direction of classification, we employ exponential moving average (EMA) (Heckert & Filliben, 2003) to integrate both past and current gradient trends:

$$\tilde{\nabla}_{\mathcal{L}_{ce}} = \alpha^T \nabla_{\mathcal{L}_{ce}}^0 + \alpha^{T-1} (1 - \alpha) \nabla_{\mathcal{L}_{ce}}^1 + \dots + (1 - \alpha) \nabla_{\mathcal{L}_{ce}}^T. \quad (11)$$

Here, α is the decay rate, $\nabla_{\mathcal{L}_{ce}}^t$ denotes the gradient of the cross-entropy loss at step t , and T represents the current step index. The GM loss is subsequently calculated as:

$$\mathcal{L}_{GM} = 1 - \cos(\tilde{\nabla}_{\mathcal{L}_{ce}}, \nabla_{\mathcal{L}_{CPT}}). \quad (12)$$

Employing the GM loss, as observed in orange dots in Fig. 3b, yields notable increases in gradient similarity across 8 of the 11 datasets, indicating a strengthened correlation between the two tasks.

4 EXPERIMENTS

4.1 EXPERIMENTAL SETUP

Datasets. We use 11 datasets covering a diverse set of recognition tasks: ImageNet (Deng et al., 2009) and Caltech101 (Fei-Fei et al., 2004) for generic object recognition, OxfordPets (Parkhi et al., 2012), StanfordCars (Krause et al., 2013), OxfordFlowers (Nilsback & Zisserman, 2008), Food101 (Bossard et al., 2014) and FGVC Aircraft (Maji et al., 2013) for fine-grained classification, SUN397 (Xiao et al., 2010) for scene recognition, DTD (Cimpoi et al., 2014) for texture classification, EuroSAT (Helber et al., 2019) for satellite recognition, and UCF101 (Soomro et al., 2012) for action recognition. Besides, four ImageNet variant datasets are involved: ImageNetV2 (Recht et al., 2019), ImageNet-Sketch (Wang et al., 2019), ImageNet-A (Hendrycks et al., 2021b) and ImageNet-R (Hendrycks et al., 2021a).

Table 2: **Cross-dataset generalization.** 16-shot ImageNet is used as the source dataset. We report top-1 accuracy (%) for each method across 10 target datasets. The best and second-best performances are highlighted in **bold red** and blue underline, respectively.

Method	Caltech	Pets	Cars	Flowers	Food101	Aircraft	SUN397	DTD	EuroSAT	UCF101	Avg.
CLIP (Radford et al., 2021)	93.35	88.25	65.48	67.44	83.65	23.67	62.59	44.27	42.01	65.13	63.58
<i>Prompt learning methods</i>											
CoOp (Zhou et al., 2022b)	93.70	89.14	64.51	68.71	85.30	18.47	64.15	41.92	46.39	66.55	63.88
CoCoOp (Zhou et al., 2022a)	94.43	90.14	65.32	71.88	86.06	22.94	67.36	45.73	45.37	68.21	65.74
KgCoOp (Yao et al., 2023)	93.92	89.83	65.41	70.01	86.36	22.51	66.16	46.35	46.04	68.50	65.51
LASP (Bulat & Tzimiropoulos, 2023)	94.50	89.36	66.20	71.74	86.40	23.03	67.00	45.54	48.50	68.24	66.05
MaPLE (Khattak et al., 2023a)	93.53	90.49	65.57	72.23	86.20	24.74	67.01	46.49	48.06	68.69	66.30
PromptSRC (Khattak et al., 2023b)	93.60	90.25	65.70	70.25	86.15	23.90	67.10	46.87	45.50	68.75	65.81
<i>LLM based methods</i>											
VisDesc (Menon & Vondrick, 2022)	<u>94.60</u>	88.85	64.08	70.85	85.05	24.30	<u>67.99</u>	44.98	<u>54.84</u>	67.12	66.27
WaffleCLIP (Roth et al., 2023)	94.02	89.95	63.57	72.35	86.68	25.39	67.23	45.21	55.07	67.19	66.67
<i>Test-time adaptation methods</i>											
TPT (Shu et al., 2022)	94.16	87.79	66.87	68.98	84.67	24.78	65.50	47.75	42.44	68.04	65.10
CoOp+TPT	93.75	88.93	<u>67.06</u>	68.25	83.82	<u>25.89</u>	66.40	47.15	48.78	66.53	65.66
MaPLE (Zhou et al., 2022b)+TPT	93.59	90.72	<u>66.50</u>	72.37	86.64	24.70	67.54	45.87	47.80	69.19	66.50
DiffTPT (Feng et al., 2023)	92.49	88.22	67.01	70.10	87.23	25.60	65.74	47.00	43.13	68.22	65.47
PromptAlign (Samadh et al., 2023)	94.01	90.76	68.50	<u>72.39</u>	86.65	24.80	67.54	47.24	47.86	69.47	66.92
Self-TPT	94.09	91.83	66.66	72.60	<u>86.89</u>	25.41	67.75	<u>49.02</u>	52.94	70.05	<u>67.72</u>
Self-TPT-v	94.71	<u>91.26</u>	68.81	71.79	85.41	27.57	68.18	49.35	51.91	<u>69.50</u>	67.85

Table 3: **Base-to-new generalization.** The 16-shot base subset of each dataset is used as the source dataset. We report top-1 accuracy (%) on each new subset to evaluate the model’s zero-shot performance to unseen classes. †: CoOp is reproduced under an identical experimental setup as ours.

Method	Generic		Fine-Grained					Specialized				Avg.
	ImageNet	Caltech	Pets	Cars	Flowers	Food101	Aircraft	SUN397	DTD	EuroSAT	UCF101	
CLIP (Radford et al., 2021)	68.14	94.00	97.26	74.89	77.80	91.22	36.29	75.35	59.90	64.05	77.50	74.22
<i>Prompt learning methods</i>												
CoOp† (Zhou et al., 2022b)	70.32	94.10	97.88	73.29	72.34	91.69	33.65	75.77	54.59	65.26	74.78	73.06
CoCoOp (Zhou et al., 2022a)	70.43	93.81	97.69	73.59	71.75	91.29	23.71	76.86	56.00	60.04	73.45	71.69
ProDA (Lu et al., 2022)	70.23	93.23	97.83	71.20	68.68	88.57	34.13	76.93	56.48	66.00	71.97	72.30
KgCoOp (Yao et al., 2023)	69.96	94.39	97.76	75.04	74.73	91.70	33.55	76.53	54.99	64.34	76.07	73.61
LoGoPrompt (Shi & Yang, 2023)	70.83	93.78	96.32	72.39	76.52	91.41	34.67	78.12	60.14	69.44	73.07	74.24
LASP (Bulat & Tzimiropoulos, 2023)	70.95	94.24	97.93	71.60	74.00	91.70	30.57	78.60	58.60	77.78	78.03	74.91
RPO (Lee et al., 2023)	71.57	94.37	97.50	75.53	76.67	90.83	34.20	77.80	62.13	68.97	75.43	75.00
CoOp+SHIP (Wang et al., 2023c)	69.95	<u>95.20</u>	97.87	73.90	74.40	91.03	32.33	75.27	56.88	66.87	76.85	73.69
MaPLE (Khattak et al., 2023a)	70.54	94.36	97.76	74.00	72.46	92.05	35.61	78.70	59.18	73.23	78.66	75.14
PromptSRC (Khattak et al., 2023b)	70.73	94.03	97.30	74.97	76.50	91.53	37.87	78.47	62.97	73.90	78.80	76.10
<i>LLM based methods</i>												
VisDesc (Menon & Vondrick, 2022)	69.84	94.54	96.53	74.45	77.52	90.49	34.55	78.48	57.97	72.44	75.34	74.74
WaffleCLIP (Roth et al., 2023)	70.36	94.31	97.32	73.39	78.87	91.77	36.13	78.03	59.04	73.38	75.73	75.30
<i>Test-time adaptation methods</i>												
TPT (Shu et al., 2022)	70.78	94.65	96.31	75.39	77.73	91.17	34.73	77.58	63.04	65.82	76.91	74.92
CoOp+TPT	72.58	94.87	97.65	75.15	72.34	91.73	36.95	77.05	58.82	64.90	69.44	73.77
MaPLE+TPT	72.24	94.29	97.37	75.20	72.10	92.03	35.81	79.18	59.91	68.96	77.34	74.95
PromptSRC+TPT	72.49	93.78	97.43	77.86	76.45	92.07	<u>38.32</u>	79.43	62.08	70.44	78.48	76.26
PromptAlign (Samadh et al., 2023)	<u>72.59</u>	94.50	97.56	75.71	72.34	92.68	37.27	<u>79.48</u>	60.55	72.71	79.30	75.88
Self-TPT	71.20	<u>95.20</u>	97.93	<u>75.89</u>	<u>78.32</u>	<u>92.09</u>	36.81	79.41	<u>63.81</u>	75.55	80.87	<u>77.01</u>
Self-TPT-v	73.40	95.49	97.15	78.08	77.99	91.46	38.33	79.92	65.14	<u>74.74</u>	<u>80.49</u>	77.47

Evaluation settings. We use three benchmarks for evaluation and report the top-1 accuracy: **(i)** Cross-data generalization: ImageNet is used as the source dataset, while the remaining 10 datasets serve as target datasets. **(ii)** Base-to-new generalization: Each dataset is divided equally into two subsets, base classes and new classes. The base subset is used as the source dataset, and the new subset is used as the target dataset for evaluation. **(iii)** Domain generalization: ImageNet is used as the source dataset, and 4 variant datasets are used as target datasets.

Implementation details. Self-TPT is built on CoOp (Zhou et al., 2022b) and is implemented on CLIP-B/16 for evaluation. All results are averaged over three seeds. We set the number of prompts M to 4. In stage 1, we use SGD as the optimizer with a learning rate of 0.002 and a batch size of 4. The prompts are trained on the source dataset in 16-shot manner. For the base-to-new setting, we train prompts for 10 epochs. For the cross-dataset and domain generalization setting, prompts are trained for 5 epochs. In stage 2, we update the prompts for 10 steps, using SGD as the optimizer with a learning rate of 0.1. Existing TPT-based methods utilize the input image and its 63 augmented views as input. To ensure a fair comparison, we also incorporate the 63 augmented images and perform an output ensemble. We refer to this specific approach as **Self-TPT-v**.

4.2 COMPARISON WITH THE STATE-OF-THE-ART METHODS

We compare Self-TPT with three kinds of methods: **i)** prompt learning methods that optimize prompts on a source dataset, **ii)** test-time prompt learning methods that adjust prompts at test time, **iii)** methods that leverage LLM (e.g., GPT-3 (Brown et al., 2020)) to produce class descriptions.

Table 5: **Ablation study of Self-TPT.** “G.”, “F.”, and “S.” represent “Generic”, “Fine-Grained”, and “Specialized” datasets, respectively, consistent with the notation used in Tab. 3. The default setting is colored grey.

(a) Main components analysis.							(b) Augmented views in CPT.							(c) Study on Gradient Matching.				
Self-TPT is built on top of CoOp.							Front	Mid	End	Hand	G.	F.	S.	EMA	Matching	G.	F.	S.
Method	CPT	TTA	GM	G.	F.	S.	✓	✓	✓	✓	83.2	76.2	74.9					
CoOp				81.8	73.8	67.6					83.0	75.8	74.4		MSE	82.8	75.6	72.2
	✓			82.3	74.9	70.5	✓		✓	✓	83.1	76.1	73.9	✓	MSE	83.1	76.1	73.9
	✓	✓		82.9	75.8	73.3				✓	83.1	75.9	73.7		Cosine	82.9	76.1	73.9
Self-TPT	✓	✓	✓	83.2	76.2	74.9	✓	✓	✓		82.9	75.9	73.6	✓	Cosine	83.2	76.2	74.9

Computational costs. Tab. 1 presents a comparison of the inference cost between Self-TPT and other TPT-based methods. Self-TPT achieves inference speeds 25 times faster than PromptAlign and 65 times faster than DiffTPT on CLIP-B/16, along with a significant reduction in graphics memory usage. Despite the use of an additional 63 augmented images, Self-TPT-v maintains a five-fold speed advantage and reduces memory usage by 15 times relative to PromptAlign. Given the rapid expansion of foundation models, the efficiency of Self-TPT highlights its potential for scalable stability in larger VLMs.

Cross-dataset generalization. In Tab. 2, we compare the performance of Self-TPT with existing state-of-the-art methods in the cross-dataset setting. Our method outperforms the previously best method on 8 out of 10 datasets, yielding an average improvement of 0.93% over PromptAlign. Note that simply combining prompt learning with test-time adaptation doesn’t always yield optimal outcomes. For instance, MaPLe+TPT shows only a slight improvement of 0.2% over MaPLe alone, suggesting that TPT may not consistently deliver significant performance improvements. Conversely, despite not being exposed to specific test images, Self-TPT still demonstrates superior performance, highlighting the effectiveness of our proposed framework.

Base-to-new generalization. In the base-to-new setting (Tab. 3), our method consistently outperforms others on 9 out of 11 datasets, achieving an average improvement of 1.37% over the previous best method, PromptSRC. Interestingly, while CoOp+TPT records a 0.71% improvement over CoOp, MaPLe+TPT shows a decline of 0.19%, again highlighting the potential unstable performance gains of TPT. Moreover, LLMs-based methods tend to fall short in complex scenarios requiring high-level understanding, *e.g.*, UCF101, which demands intricate human action comprehension.

Domain generalization. We present Self-TPT’s results on four ImageNet variant datasets with domain shifts in Tab. 4. Remarkably, Self-TPT set new state-of-the-art records on three of these datasets, demonstrating its robustness to domain shifts and adaptability to varying image distributions. Although Self-TPT was outperformed by CoOp+TPT and CoOp+DiffTPT on ImageNet-V2, we speculate this is because ImageNet-V2’s data distribution closely aligns with that of ImageNet, the source dataset. CoOp is well-known for overfitting on source data.

Table 4: **Domain generalization.** ImageNet is used as source data. “Aug” indicates the original image is augmented 63 times and input jointly.

Method	Aug	IN-V2	IN-Sk.	IN-A	IN-R	Avg.
CLIP		60.86	46.09	47.87	73.98	57.20
TPT	✓	63.45	47.94	54.77	77.06	60.81
CoOp+TPT	✓	66.83	49.29	57.95	77.27	62.84
MaPLe+TPT	✓	64.87	48.16	58.08	78.12	62.31
DiffTPT	✓	65.10	46.80	55.68	75.00	60.65
CoOp+DiffTPT	✓	66.80	49.50	58.09	73.90	62.07
PromptAlign	✓	65.29	50.23	59.37	79.33	63.56
Self-TPT-v	✓	66.55	51.72	63.48	79.76	65.38

4.3 ABLATION STUDY

Main components analysis. In developing Self-TPT based on CoOp, we made three key progress. First, we integrated CPT during the source prompt learning phase. This integration aims to cultivate more robust and generalizable feature representations. Second, we applied CPT during test-time adaptation, improving the understanding of the new class prior to the prediction phase. Lastly, we incorporated the GM loss in the source prompt learning stage to explicitly strengthen the gradient correlation between CPT and the classification task. The effectiveness of each component is quantitatively assessed in Tab. 5a. The results demonstrate that each component of Self-TPT contributes to consistent performance improvements across the board.

Study on different views in CPT. As shown in Fig. 3a, Self-TPT employs four distinct views per class for contrastive learning. In Tab. 5b, we perform an ablation study by sequentially removing one view at a time, which results in a consistent decline in performance. The degradation becomes

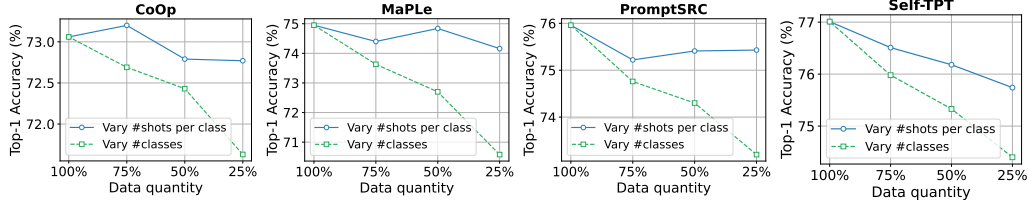


Figure 4: Study on source data quality: more classes or more shots?

Table 6: Study on model versatility.

(a) Comparison on different model architectures and scales.

Model	ResNet		VisionTransformer		
	RN50	RN101	B/32	B/16	L/14
CLIP (Radford et al., 2021)	68.72	69.90	71.80	74.22	80.34
CoOp (Zhou et al., 2022b)	66.75	68.98	70.26	73.06	78.97
WaffleCLIP (Roth et al., 2023)	69.04	70.06	72.30	75.30	81.12
Self-TPT	70.90	71.94	73.83	77.01	82.13

(b) Self-TPT generalizes to a different VLM.

Method	Acc.
EVA-CLIP (Sun et al., 2023)	77.33
EVA-CLIP + CoOp (Zhou et al., 2022b)	75.68
EVA-CLIP + PromptSRC (Khattak et al., 2023b)	78.68
EVA-CLIP + VisDesc (Menon & Vondrick, 2022)	78.12
EVA-CLIP + WaffleCLIP (Roth et al., 2023)	78.59
EVA-CLIP + Self-TPT	79.81

more pronounced when two views are removed. These findings suggest that incorporating multiple views enhances the effectiveness of the contrastive prompt tuning task.

Study on gradient matching. Tab. 5c presents the results of the ablation study on the gradient matching (GM) loss. We replaced the cosine similarity loss with mean square error (MSE) in Eq. 12 and observed a decrease in effectiveness. This indicates that enforcing exact numerical equality of gradients from two different tasks may be impractical. Additionally, we assessed the impact of using exponential moving average (EMA) and found consistent improvements, underscoring that maintaining a robust gradient direction is critical for the effectiveness of GM loss.

Study on source data quantity and quality. Source data is pivotal in both prompt learning and TPT-based methods. In Tab. 7, we examine the impact of reducing data quantity on model performance. The analysis encompasses 25%, 50%, 75%, and 100% of the default data volume. Our findings indicate that Self-TPT maintains robust performance even with limited source data, highlighting its efficiency in data utilization. Furthermore, we address a critical question: *Is it more beneficial to have more classes or more instances per class?* This inquiry involves varying both the number of shots per class and the number of classes. The performance outcomes of four methods are depicted in Fig. 4. The results reveal a significant performance decline with a reduced number of classes, underscoring the importance of prioritizing class diversity in data collection for real-world applications.

Study on model versatility. In Tab. 6a, we adapt Self-TPT to various backbone architectures, including ResNet (He et al., 2016) and ViT (Dosovitskiy et al., 2020), across different scales. Notably, Self-TPT consistently delivers performance improvements across all tested backbones, demonstrating its broad applicability and robust effectiveness. Besides, we extend the application of Self-TPT and several competitive methods to another VLM, EVA-CLIP (Sun et al., 2023), as shown in Tab. 6b. Once again, Self-TPT demonstrates distinct advantages over competing methods, further confirming its effectiveness and versatility.

Table 7: Model performance with reduced data quantity.

Method	25%	50%	75%	100%
CoOp	71.63	72.43	72.69	73.06
MaPLE	70.58	72.70	73.63	74.95
PromptSRC	73.20	74.30	74.76	75.96
Self-TPT	74.40	75.33	75.98	77.01

5 CONCLUSION

In this paper, we introduced Self-TPT, a novel framework for efficient test-time prompt tuning. Self-TPT resolves the inefficiencies in inference observed with existing TPT-based methods by incorporating text-oriented self-supervised learning for new class adaptation, converting per-image adaptation into a preprocessing step. We introduced a novel contrastive prompt tuning (CPT) task for self-supervision. Empirical results demonstrate that CPT has a positive gradient correlation with classification tasks, explaining its effectiveness. Based on these findings, we proposed a gradient matching loss to enhance this correlation further. Extensive testing on three benchmarks confirmed the effectiveness and efficiency of our method.

REFERENCES

- Jean-Baptiste Alayrac, Jeff Donahue, Pauline Luc, Antoine Miech, Iain Barr, Yana Hasson, Karel Lenc, Arthur Mensch, Katherine Millican, Malcolm Reynolds, et al. Flamingo: a visual language model for few-shot learning. *Advances in Neural Information Processing Systems*, 35:23716–23736, 2022.
- Lukas Bossard, Matthieu Guillaumin, and Luc Van Gool. Food-101—mining discriminative components with random forests. In *ECCV*, pp. 446–461, 2014.
- Tom Brown, Benjamin Mann, Nick Ryder, Melanie Subbiah, Jared D Kaplan, Prafulla Dhariwal, Arvind Neelakantan, Pranav Shyam, Girish Sastry, Amanda Askell, et al. Language models are few-shot learners. *Advances in neural information processing systems*, 33:1877–1901, 2020.
- Adrian Bulat and Georgios Tzimiropoulos. Laspl: Text-to-text optimization for language-aware soft prompting of vision & language models. In *Proceedings of the IEEE/CVF Conference on Computer Vision and Pattern Recognition*, pp. 23232–23241, 2023.
- Joao Carreira, Eric Noland, Andras Banki-Horvath, Chloe Hillier, and Andrew Zisserman. A short note about kinetics-600. *arXiv preprint arXiv:1808.01340*, 2018.
- Dian Chen, Dequan Wang, Trevor Darrell, and Sayna Ebrahimi. Contrastive test-time adaptation. In *Proceedings of the IEEE/CVF Conference on Computer Vision and Pattern Recognition*, pp. 295–305, 2022a.
- Guangyi Chen, Weiran Yao, Xiangchen Song, Xinyue Li, Yongming Rao, and Kun Zhang. Prompt learning with optimal transport for vision-language models. *arXiv preprint arXiv:2210.01253*, 2022b.
- Liang Chen, Yong Zhang, Yibing Song, Ying Shan, and Lingqiao Liu. Improved test-time adaptation for domain generalization. In *Proceedings of the IEEE/CVF Conference on Computer Vision and Pattern Recognition*, pp. 24172–24182, 2023.
- Shizhe Chen and Dong Huang. Elaborative rehearsal for zero-shot action recognition. In *Proceedings of the IEEE/CVF International Conference on Computer Vision*, pp. 13638–13647, 2021.
- Shoufa Chen, Chongjian Ge, Zhan Tong, Jiangliu Wang, Yibing Song, Jue Wang, and Ping Luo. Adapformer: Adapting vision transformers for scalable visual recognition. *Advances in Neural Information Processing Systems*, 35:16664–16678, 2022c.
- Ting Chen, Simon Kornblith, Mohammad Norouzi, and Geoffrey Hinton. A simple framework for contrastive learning of visual representations. In *International conference on machine learning*, pp. 1597–1607. PMLR, 2020.
- Mircea Cimpoi, Subhransu Maji, Iasonas Kokkinos, Sammy Mohamed, and Andrea Vedaldi. Describing textures in the wild. In *CVPR*, pp. 3606–3613, 2014.
- Jia Deng, Wei Dong, Richard Socher, Li-Jia Li, Kai Li, and Li Fei-Fei. Imagenet: A large-scale hierarchical image database. In *CVPR*, pp. 248–255, 2009.
- Alexey Dosovitskiy, Lucas Beyer, Alexander Kolesnikov, Dirk Weissenborn, Xiaohua Zhai, Thomas Unterthiner, Mostafa Dehghani, Matthias Minderer, Georg Heigold, Sylvain Gelly, et al. An image is worth 16x16 words: Transformers for image recognition at scale. *arXiv preprint arXiv:2010.11929*, 2020.
- Yu Du, Fangyun Wei, Zihe Zhang, Miaojing Shi, Yue Gao, and Guoqi Li. Learning to prompt for open-vocabulary object detection with vision-language model. In *Proceedings of the IEEE/CVF Conference on Computer Vision and Pattern Recognition*, pp. 14084–14093, 2022.
- Yuxin Fang, Wen Wang, Binhui Xie, Quan Sun, Ledell Wu, Xinggang Wang, Tiejun Huang, Xinlong Wang, and Yue Cao. Eva: Exploring the limits of masked visual representation learning at scale. In *Proceedings of the IEEE/CVF Conference on Computer Vision and Pattern Recognition*, pp. 19358–19369, 2023.

- Li Fei-Fei, Rob Fergus, and Pietro Perona. Learning generative visual models from few training examples: An incremental bayesian approach tested on 101 object categories. In *CVPR-W*, pp. 178–178, 2004.
- Chun-Mei Feng, Kai Yu, Yong Liu, Salman Khan, and Wangmeng Zuo. Diverse data augmentation with diffusions for effective test-time prompt tuning. *arXiv preprint arXiv:2308.06038*, 2023.
- Yossi Gandelsman, Yu Sun, Xinlei Chen, and Alexei Efros. Test-time training with masked autoencoders. *Advances in Neural Information Processing Systems*, 35:29374–29385, 2022.
- Xavier Glorot and Yoshua Bengio. Understanding the difficulty of training deep feedforward neural networks. In *AISTATS*, pp. 249–256, 2010.
- Kaiming He, Xiangyu Zhang, Shaoqing Ren, and Jian Sun. Deep residual learning for image recognition. In *Proceedings of the IEEE conference on computer vision and pattern recognition*, pp. 770–778, 2016.
- Kaiming He, Haoqi Fan, Yuxin Wu, Saining Xie, and Ross Girshick. Momentum contrast for unsupervised visual representation learning. In *Proceedings of the IEEE/CVF conference on computer vision and pattern recognition*, pp. 9729–9738, 2020.
- N. Heckert and James Filliben. Nist/sematech e-handbook of statistical methods, 2003-06-01 00:06:00 2003.
- Patrick Helber, Benjamin Bischke, Andreas Dengel, and Damian Borth. Eurosat: A novel dataset and deep learning benchmark for land use and land cover classification. *IEEE Journal of Selected Topics in Applied Earth Observations and Remote Sensing*, 12(7):2217–2226, 2019.
- Dan Hendrycks, Steven Basart, Norman Mu, Saurav Kadavath, Frank Wang, Evan Dorundo, Rahul Desai, Tyler Zhu, Samyak Parajuli, Mike Guo, et al. The many faces of robustness: A critical analysis of out-of-distribution generalization. In *Proceedings of the IEEE/CVF International Conference on Computer Vision*, pp. 8340–8349, 2021a.
- Dan Hendrycks, Kevin Zhao, Steven Basart, Jacob Steinhardt, and Dawn Song. Natural adversarial examples. In *Proceedings of the IEEE/CVF Conference on Computer Vision and Pattern Recognition*, pp. 15262–15271, 2021b.
- Jiaxing Huang, Dayan Guan, Aoran Xiao, and Shijian Lu. Model adaptation: Historical contrastive learning for unsupervised domain adaptation without source data. *Advances in Neural Information Processing Systems*, 34:3635–3649, 2021.
- Xiaohu Huang, Hao Zhou, Kun Yao, and Kai Han. Froster: Frozen clip is a strong teacher for open-vocabulary action recognition. *arXiv preprint arXiv:2402.03241*, 2024.
- Chao Jia, Yinfei Yang, Ye Xia, Yi-Ting Chen, Zarana Parekh, Hieu Pham, Quoc Le, Yun-Hsuan Sung, Zhen Li, and Tom Duerig. Scaling up visual and vision-language representation learning with noisy text supervision. In *International conference on machine learning*, pp. 4904–4916. PMLR, 2021.
- Baoshuo Kan, Teng Wang, Wenpeng Lu, Xiantong Zhen, Weili Guan, and Feng Zheng. Knowledge-aware prompt tuning for generalizable vision-language models. *arXiv preprint arXiv:2308.11186*, 2023.
- Will Kay, Joao Carreira, Karen Simonyan, Brian Zhang, Chloe Hillier, Sudheendra Vijayanarasimhan, Fabio Viola, Tim Green, Trevor Back, Paul Natsev, et al. The kinetics human action video dataset. *arXiv preprint arXiv:1705.06950*, 2017.
- Muhammad Uzair Khattak, Hanoona Rasheed, Muhammad Maaz, Salman Khan, and Fahad Shahbaz Khan. Maple: Multi-modal prompt learning. In *Proceedings of the IEEE/CVF Conference on Computer Vision and Pattern Recognition*, pp. 19113–19122, 2023a.
- Muhammad Uzair Khattak, Syed Talal Wasim, Muzammal Naseer, Salman Khan, Ming-Hsuan Yang, and Fahad Shahbaz Khan. Self-regulating prompts: Foundational model adaptation without forgetting. *arXiv preprint arXiv:2307.06948*, 2023b.

- Prannay Khosla, Piotr Teterwak, Chen Wang, Aaron Sarna, Yonglong Tian, Phillip Isola, Aaron Maschinot, Ce Liu, and Dilip Krishnan. Supervised contrastive learning. *Advances in neural information processing systems*, 33:18661–18673, 2020.
- Jonathan Krause, Michael Stark, Jia Deng, and Li Fei-Fei. 3d object representations for fine-grained categorization. In *ICCV-W*, pp. 554–561. IEEE, 2013.
- Hildegard Kuehne, Hueihan Jhuang, Estíbaliz Garrote, Tomaso Poggio, and Thomas Serre. Hmdb: a large video database for human motion recognition. In *2011 International conference on computer vision*, pp. 2556–2563. IEEE, 2011.
- Dongjun Lee, Seokwon Song, Jihee Suh, Joonmyeong Choi, Sanghyeok Lee, and Hyunwoo J Kim. Read-only prompt optimization for vision-language few-shot learning. *arXiv preprint arXiv:2308.14960*, 2023.
- Junnan Li, Dongxu Li, Caiming Xiong, and Steven Hoi. Blip: Bootstrapping language-image pre-training for unified vision-language understanding and generation. In *International Conference on Machine Learning*, pp. 12888–12900. PMLR, 2022.
- Xinhao Li, Yuhan Zhu, and Limin Wang. Zeroi2v: Zero-cost adaptation of pre-trained transformers from image to video. *arXiv preprint arXiv:2310.01324*, 2023.
- Jian Liang, Dapeng Hu, and Jiashi Feng. Do we really need to access the source data? source hypothesis transfer for unsupervised domain adaptation. In *International conference on machine learning*, pp. 6028–6039. PMLR, 2020a.
- Jian Liang, Dapeng Hu, and Jiashi Feng. Do we really need to access the source data? source hypothesis transfer for unsupervised domain adaptation. In *International conference on machine learning*, pp. 6028–6039. PMLR, 2020b.
- Haotian Liu, Chunyuan Li, Qingyang Wu, and Yong Jae Lee. Visual instruction tuning. *Advances in neural information processing systems*, 36, 2024.
- Yuejiang Liu, Parth Kothari, Bastien Van Delft, Baptiste Bellot-Gurlet, Taylor Mordan, and Alexandre Alahi. Ttt++: When does self-supervised test-time training fail or thrive? *Advances in Neural Information Processing Systems*, 34:21808–21820, 2021.
- Sifan Long, Zhen Zhao, Junkun Yuan, Zichang Tan, Jiangjiang Liu, Luping Zhou, Shengsheng Wang, and Jingdong Wang. Task-oriented multi-modal mutual learning for vision-language models. *arXiv preprint arXiv:2303.17169*, 2023.
- Yuning Lu, Jianzhuang Liu, Yonggang Zhang, Yajing Liu, and Xinmei Tian. Prompt distribution learning. In *Proceedings of the IEEE/CVF Conference on Computer Vision and Pattern Recognition*, pp. 5206–5215, 2022.
- Xiaosong Ma, Jie ZHANG, Song Guo, and Wenchao Xu. Swapprompt: Test-time prompt adaptation for vision-language models. In *Thirty-seventh Conference on Neural Information Processing Systems*, 2023. URL <https://openreview.net/forum?id=EhdNQiOWgQ>.
- Subhransu Maji, Esa Rahtu, Juho Kannala, Matthew Blaschko, and Andrea Vedaldi. Fine-grained visual classification of aircraft, 2013.
- Sachit Menon and Carl Vondrick. Visual classification via description from large language models. In *The Eleventh International Conference on Learning Representations*, 2022.
- Matthias Minderer, Alexey Gritsenko, Austin Stone, Maxim Neumann, Dirk Weissenborn, Alexey Dosovitskiy, Aravindh Mahendran, Anurag Arnab, Mostafa Dehghani, Zhuoran Shen, et al. Simple open-vocabulary object detection. In *European Conference on Computer Vision*, pp. 728–755. Springer, 2022.
- Maria-Elena Nilsback and Andrew Zisserman. Automated flower classification over a large number of classes. In *ICVGIP*, pp. 722–729, 2008.

- Shuaicheng Niu, Jiaxiang Wu, Yifan Zhang, Zhiquan Wen, Yaofo Chen, Peilin Zhao, and Mingkui Tan. Towards stable test-time adaptation in dynamic wild world. *arXiv preprint arXiv:2302.12400*, 2023.
- Junting Pan, Ziyi Lin, Xiatian Zhu, Jing Shao, and Hongsheng Li. St-adapter: Parameter-efficient image-to-video transfer learning. *Advances in Neural Information Processing Systems*, 35:26462–26477, 2022.
- Omkar M Parkhi, Andrea Vedaldi, Andrew Zisserman, and CV Jawahar. Cats and dogs. In *CVPR*, pp. 3498–3505, 2012.
- Alec Radford, Jong Wook Kim, Chris Hallacy, Aditya Ramesh, Gabriel Goh, Sandhini Agarwal, Girish Sastry, Amanda Askell, Pamela Mishkin, Jack Clark, et al. Learning transferable visual models from natural language supervision. In *International conference on machine learning*, pp. 8748–8763. PMLR, 2021.
- Benjamin Recht, Rebecca Roelofs, Ludwig Schmidt, and Vaishal Shankar. Do imagenet classifiers generalize to imagenet? In *International conference on machine learning*, pp. 5389–5400. PMLR, 2019.
- Robin Rombach, Andreas Blattmann, Dominik Lorenz, Patrick Esser, and Björn Ommer. High-resolution image synthesis with latent diffusion models. In *Proceedings of the IEEE/CVF conference on computer vision and pattern recognition*, pp. 10684–10695, 2022.
- Karsten Roth, Jae Myung Kim, A Koepke, Oriol Vinyals, Cordelia Schmid, and Zeynep Akata. Waffling around for performance: Visual classification with random words and broad concepts. *arXiv preprint arXiv:2306.07282*, 2023.
- Jameel Hassan Abdul Samadh, Hanan Gani, Noor Hazim Hussein, Muhammad Uzair Khattak, Muzammal Naseer, Fahad Khan, and Salman Khan. Align your prompts: Test-time prompting with distribution alignment for zero-shot generalization. In *Thirty-seventh Conference on Neural Information Processing Systems*, 2023. URL <https://openreview.net/forum?id=CusNOTRkQw>.
- Cheng Shi and Sibe Yang. Logoprompt: Synthetic text images can be good visual prompts for vision-language models. *arXiv preprint arXiv:2309.01155*, 2023.
- Taylor Shin, Yasaman Razeghi, Robert L Logan IV, Eric Wallace, and Sameer Singh. Autoprompt: Eliciting knowledge from language models with automatically generated prompts. *arXiv preprint arXiv:2010.15980*, 2020.
- Manli Shu, Weili Nie, De-An Huang, Zhiding Yu, Tom Goldstein, Anima Anandkumar, and Chaowei Xiao. Test-time prompt tuning for zero-shot generalization in vision-language models. *Advances in Neural Information Processing Systems*, 35:14274–14289, 2022.
- Mainak Singha, Ankit Jha, and Biplab Banerjee. Gopro: Generate and optimize prompts in clip using self-supervised learning. *arXiv preprint arXiv:2308.11605*, 2023.
- Khurram Soomro, Amir Roshan Zamir, and Mubarak Shah. Ucf101: A dataset of 101 human actions classes from videos in the wild, 2012.
- Quan Sun, Yuxin Fang, Ledell Wu, Xinlong Wang, and Yue Cao. Eva-clip: Improved training techniques for clip at scale. *arXiv preprint arXiv:2303.15389*, 2023.
- Yu Sun, Xiaolong Wang, Zhuang Liu, John Miller, Alexei Efros, and Moritz Hardt. Test-time training with self-supervision for generalization under distribution shifts. In *International conference on machine learning*, pp. 9229–9248. PMLR, 2020.
- Dequan Wang, Evan Shelhamer, Shaoteng Liu, Bruno Olshausen, and Trevor Darrell. Tent: Fully test-time adaptation by entropy minimization. *arXiv preprint arXiv:2006.10726*, 2020.
- Dongsheng Wang, Miaoge Li, Xinyang Liu, MingSheng Xu, Bo Chen, and Hanwang Zhang. Tuning multi-mode token-level prompt alignment across modalities. In *Thirty-seventh Conference on Neural Information Processing Systems*, 2023a. URL <https://openreview.net/forum?id=A253n2EXCd>.

- Haohan Wang, Songwei Ge, Zachary Lipton, and Eric P Xing. Learning robust global representations by penalizing local predictive power. *Advances in Neural Information Processing Systems*, 32, 2019.
- Jun-Kun Wang and Andre Wibisono. Towards understanding gd with hard and conjugate pseudo-labels for test-time adaptation. *arXiv preprint arXiv:2210.10019*, 2022.
- Mengmeng Wang, Jiazheng Xing, and Yong Liu. Actionclip: A new paradigm for video action recognition. *arXiv preprint arXiv:2109.08472*, 2021.
- Shuai Wang, Daoan Zhang, Zipei Yan, Jianguo Zhang, and Rui Li. Feature alignment and uniformity for test time adaptation. In *Proceedings of the IEEE/CVF Conference on Computer Vision and Pattern Recognition*, pp. 20050–20060, 2023b.
- Xi Wang and Laurence Aitchison. Robustness to corruption in pre-trained bayesian neural networks. In *The Eleventh International Conference on Learning Representations*, 2022.
- Zhengbo Wang, Jian Liang, Ran He, Nan Xu, Zilei Wang, and Tieniu Tan. Improving zero-shot generalization for clip with synthesized prompts. *arXiv preprint arXiv:2307.07397*, 2023c.
- ZeJia Weng, Xitong Yang, Ang Li, Zuxuan Wu, and Yu-Gang Jiang. Open-vclip: Transforming clip to an open-vocabulary video model via interpolated weight optimization. In *ICML*, 2023.
- Wenhao Wu, Zhun Sun, Yuxin Song, Jingdong Wang, and Wanli Ouyang. Transferring vision-language models for visual recognition: A classifier perspective. *International Journal of Computer Vision*, pp. 1–18, 2023.
- Jianxiong Xiao, James Hays, Krista A Ehinger, Aude Oliva, and Antonio Torralba. Sun database: Large-scale scene recognition from abbey to zoo. In *CVPR*, pp. 3485–3492, 2010.
- Chen Xu, Yuhan Zhu, Haocheng Shen, Boheng Chen, Yixuan Liao, Xiaoxin Chen, and Limin Wang. Progressive visual prompt learning with contrastive feature re-formation. *arXiv preprint arXiv:2304.08386*, 2023a.
- Chen Xu, Yuhan Zhu, Guozhen Zhang, Haocheng Shen, Yixuan Liao, Xiaoxin Chen, Gangshan Wu, and Limin Wang. Dpl: Decoupled prompt learning for vision-language models. *arXiv preprint arXiv:2308.10061*, 2023b.
- Taojiannan Yang, Yi Zhu, Yusheng Xie, Aston Zhang, Chen Chen, and Mu Li. Aim: Adapting image models for efficient video action recognition. *arXiv preprint arXiv:2302.03024*, 2023.
- Hantao Yao, Rui Zhang, and Changsheng Xu. Visual-language prompt tuning with knowledge-guided context optimization. In *Proceedings of the IEEE/CVF Conference on Computer Vision and Pattern Recognition*, pp. 6757–6767, 2023.
- Yuhang Zang, Wei Li, Kaiyang Zhou, Chen Huang, and Chen Change Loy. Unified vision and language prompt learning. *arXiv preprint arXiv:2210.07225*, 2022.
- Xiaohua Zhai, Xiao Wang, Basil Mustafa, Andreas Steiner, Daniel Keysers, Alexander Kolesnikov, and Lucas Beyer. Lit: Zero-shot transfer with locked-image text tuning. In *Proceedings of the IEEE/CVF Conference on Computer Vision and Pattern Recognition*, pp. 18123–18133, 2022.
- Guozhen Zhang, Yuhan Zhu, Haonan Wang, Youxin Chen, Gangshan Wu, and Limin Wang. Extracting motion and appearance via inter-frame attention for efficient video frame interpolation. In *Proceedings of the IEEE/CVF Conference on Computer Vision and Pattern Recognition*, pp. 5682–5692, 2023.
- Bowen Zhao, Chen Chen, and Shu-Tao Xia. Delta: degradation-free fully test-time adaptation. *arXiv preprint arXiv:2301.13018*, 2023.
- Zexuan Zhong, Dan Friedman, and Danqi Chen. Factual probing is [mask]: Learning vs. learning to recall. *arXiv preprint arXiv:2104.05240*, 2021.

- Kaiyang Zhou, Jingkang Yang, Chen Change Loy, and Ziwei Liu. Conditional prompt learning for vision-language models. In *Proceedings of the IEEE/CVF Conference on Computer Vision and Pattern Recognition*, pp. 16816–16825, 2022a.
- Kaiyang Zhou, Jingkang Yang, Chen Change Loy, and Ziwei Liu. Learning to prompt for vision-language models. *International Journal of Computer Vision*, 130(9):2337–2348, 2022b.
- Beier Zhu, Yulei Niu, Yucheng Han, Yue Wu, and Hanwang Zhang. Prompt-aligned gradient for prompt tuning. *arXiv preprint arXiv:2205.14865*, 2022.
- Deyao Zhu, Jun Chen, Xiaoqian Shen, Xiang Li, and Mohamed Elhoseiny. Minigpt-4: Enhancing vision-language understanding with advanced large language models. *arXiv preprint arXiv:2304.10592*, 2023.
- Yuhan Zhu, Yuyang Ji, Zhiyu Zhao, Gangshan Wu, and Limin Wang. Awt: Transferring vision-language models via augmentation, weighting, and transportation. *arXiv preprint arXiv:2407.04603*, 2024a.
- Yuhan Zhu, Guozhen Zhang, Jing Tan, Gangshan Wu, and Limin Wang. Dual detr for multi-label temporal action detection. In *Proceedings of the IEEE/CVF Conference on Computer Vision and Pattern Recognition*, pp. 18559–18569, 2024b.

A ADDITIONAL DETAILS

Datasets Details. Tab. 8 presents an overview of the 14 datasets utilized in the main paper. In line with CoOp (Zhou et al., 2022b), the classes “BACKGROUND_Google” and “Faces easy” are excluded from the Caltech101 dataset. As for the video dataset UCF101, we use the middle frame of each video as the input.

Table 8: **Datasets statistics.**

Dataset	Classes	Train	Validation	Test
ImageNet (Deng et al., 2009)	1,000	1.28M	N/A	50,000
Caltech101 (Fei-Fei et al., 2004)	100	4,128	1,649	2,465
OxfordPets (Parkhi et al., 2012)	37	2,944	736	3,669
StanfordCars (Krause et al., 2013)	196	6,509	1,635	8,041
Flowers102 (Nilsback & Zisserman, 2008)	102	4,093	1,633	2,463
Food101 (Bossard et al., 2014)	101	50,500	20,200	30,300
FGVCAircraft (Maji et al., 2013)	100	3,334	3,333	3,333
SUN397 (Xiao et al., 2010)	397	15,880	3,970	19,850
DTD (Cimpoi et al., 2014)	47	2,820	1,128	1,692
EuroSAT (Helber et al., 2019)	10	13,500	5,400	8,100
UCF101 (Soomro et al., 2012)	101	7,639	1,898	3,783
ImageNetV2 (Recht et al., 2019)	1,000	N/A	N/A	10,000
ImageNet-Sketch (Wang et al., 2019)	1,000	N/A	N/A	50,889
ImageNet-A (Hendrycks et al., 2021b)	200	N/A	N/A	7,500
ImageNet-R (Hendrycks et al., 2021a)	200	N/A	N/A	30,000

Additional Implementation Details. The learnable prompts are initialized with pre-trained CLIP word embeddings of “a photo of a” at the beginning of stage 1. To eliminate the need for an additional validation set, we opt to select the model at the last step of both stage 1 and stage 2. Consistent with prior research (Zhou et al., 2022b;a; Zhu et al., 2022; Khattak et al., 2023a), training at stage 1 includes techniques such as random resized cropping and flipping. We also implement a warm-up strategy where the learning rate is initially set at $1e - 5$ for the first epoch, and then it follows a cosine annealing schedule starting from $2e - 3$. For the projection head, we employ a nonlinear projection similar to (Chen et al., 2020; Khosla et al., 2020), which incorporates an additional hidden layer with ReLU activation. By default, the projection dimension is set to 128. We initialize the weights of the projection head using the Xavier (Glorot & Bengio, 2010) and set the bias to 0. All experiments are conducted on a single A100 GPU.

B ADDITIONAL STUDIES

Study on hyperparameter sensitivity. In Fig. 5, we present a sensitivity analysis of Self-TPT by exploring variations in the number of update steps and learning rates during the test-time adaptation phase. Notably, Self-TPT maintained robust performance across various adaptation steps, with a preference for higher learning rates to optimize its effectiveness.

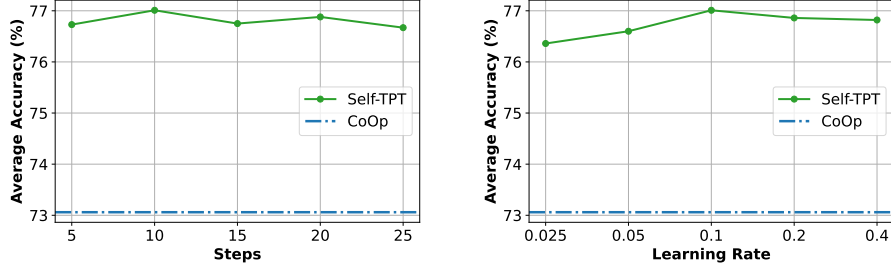


Figure 5: Study on Hyperparameter Sensitivity.

Error bar analysis. Error bar analysis was performed across both cross-dataset and base-to-new settings using three different seeds. The mean and standard deviation values are presented in Tab. 9 and Tab. 10. It was observed that, in most datasets, Self-TPT demonstrates a minimal performance divergence. Notably, EuroSAT, which has a limited number of classes, exhibited significant sensitivity in performance outcomes.

Table 9: **Error Bar** on cross-dataset generalization.

Method	Caltech	Pets	Cars	Flowers	Food101
CLIP	93.35	88.25	65.48	67.44	83.65
CoOp	93.70	89.14	64.51	68.71	85.30
Self-TPT	94.09±0.17	91.83±0.26	66.66±0.38	72.60±0.29	86.89±0.10

Method	Aircraft	SUN397	DTD	EuroSAT	UCF101	Avg.
CLIP	23.67	62.59	44.27	42.01	65.13	63.58
CoOp	18.47	64.15	41.92	46.39	66.55	63.88
Self-TPT	25.41±0.45	67.75±0.04	49.02±0.29	52.94±2.42	70.05±0.06	67.73±0.18

Table 10: **Error Bar** on base-to-new generalization.

Method	ImageNet	Caltech	Pets	Cars	Flowers	Food101
CLIP	68.14	94.00	97.26	74.89	77.80	91.22
CoOp	70.32	94.10	97.88	73.29	72.34	91.69
Self-TPT	71.20±0.02	95.20±0.18	97.93±0.20	75.89±0.62	78.32±0.44	92.09±0.20

Method	Aircraft	SUN397	DTD	EuroSAT	UCF101	Avg.
CLIP	36.29	75.35	59.90	64.05	77.50	74.22
CoOp	33.65	75.77	54.59	65.26	74.78	73.06
Self-TPT	36.81±0.14	79.41±0.28	63.81±0.41	75.55±0.82	80.87±0.42	77.01±0.11

Visualization of CPT. We employ t-SNE to visualize text embeddings and observe that embeddings generated using CPT demonstrate a distinct manifold structure, which is not apparent in the original embeddings. Additionally, an analysis of cosine distances between text embeddings indicates that CPT significantly enhances differentiation between classes.

Extending Self-TPT to zero-shot video recognition We assess the performance of Self-TPT in the realm of zero-shot video recognition. Following Open-VCLIP (Weng et al., 2023), we evaluate our model using the full UCF101 (Soomro et al., 2012) and HMDB51 (Kuehne et al., 2011) test sets, along with three selected subsets of Kinetics-600 (Carreira et al., 2018), as segmented by Chen & Huang (2021). Similar to Open-VCLIP, we incorporate neighbor-frame attention to model the temporal dynamics and train the CLIP image encoder on Kinetics-400 (Kay et al., 2017). It is important to note that the three subsets of Kinetics-600 have distinct class sets compared to Kinetics-400. For text prompts, we employ Self-TPT’s prompts optimized on 16-shot ImageNet and then

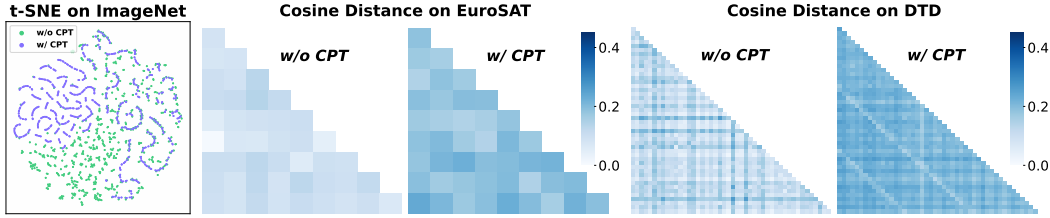


Figure 6: **Visualization of text embeddings.** We present a t-SNE visualization on the ImageNet dataset, consisting of 1000 classes, and compute the cosine distance between text embeddings from EuroSAT and DTD. Darker colors indicate a greater distance.

adapt them to the action classes at test time. The evaluation results are summarized in Tab. 11. Remarkably, Self-TPT surpasses the performance of the state-of-the-art Open-VCLIP by margins of 0.9%, 2.0%, and 0.7% across the respective datasets.

Table 11: **Extending Self-TPT to zero-shot video recognition.**

Method	UCF101	HMDB51	Kinetics-600
CLIP (Radford et al., 2021)	74.2	46.3	68.1 \pm 1.1
ActionCLIP (Wang et al., 2021)	77.4	48.0	62.5 \pm 1.2
Text4Vis (Wu et al., 2023)	76.4	44.5	60.1 \pm 0.5
AdapterFormer (Chen et al., 2022c)	80.5	50.5	67.0 \pm 0.4
AIM (Yang et al., 2023)	79.0	49.5	66.7 \pm 0.5
ST-Adapter (Pan et al., 2022)	77.9	50.3	60.2 \pm 1.8
Open-VCLIP (Weng et al., 2023)	83.5	53.2	73.0 \pm 0.8
Self-TPT	84.4	55.2	73.7\pm0.8

C LIMITATIONS AND FUTURE WORK

Although existing TTA techniques show promise and effectiveness, their computational costs hinder their deployment in real-world scenarios. Self-TPT takes a stride forward by turning specific-sample adaptation into a pre-processing step. However, the extra costs brought by the nature of test-time adaptation still exist. There is a risk for Self-TPT degrading to vanilla TPT scenarios when the samples come with different class sets. In the future, our objectives include refining the Self-TPT framework to better align with practical applications. We also intend to investigate the potential of test-time prompt tuning across various other fields, such as video understanding (Zhu et al., 2024b; Zhang et al., 2023; Li et al., 2023) and more intricate visual-language tasks (Liu et al., 2024; Zhu et al., 2023).

D PSEUDO CODE

In Algo. 1, we present the pseudo-code for Self-TPT. The definitions of the symbols are consistent with those in the main paper.

Algorithm 1 Self-TPT: Test-time Prompt Tuning with Self-supervision

Input: Source data $\mathcal{S} = (\mathcal{X}^{(s)}, \mathcal{Y}^{(s)}, \mathcal{M}^{(s)})$, target data $\mathcal{T} = (\mathcal{X}^{(t)}, \mathcal{Y}^{(t)})$
Output: Label index $I = (I_1, I_2, \dots)$

Stage 1: Prompt Learning

for $T = 1, 2, \dots$ **do**

Sample batch $(\mathcal{X}_i^{(s)}, \mathcal{M}_i^{(s)}) \sim (\mathcal{X}^{(s)}, \mathcal{M}^{(s)})$

$\mathbf{t} \leftarrow \mathcal{Y}^{(s)}, \mathbf{P}$ # combine class token with prompts

$\mathbf{e} \leftarrow f(\mathcal{X}_i^{(s)}), \mathbf{w} \leftarrow g(\mathbf{t}), \mathbf{z} \leftarrow h(\mathbf{w})$ # compute image and text features

$\mathcal{L}_{ce} \leftarrow \mathcal{L}_{ce}(\cos(\mathbf{e}, \mathbf{w}), \mathcal{M}_i^{(s)})$ # supervised loss

$\mathcal{L}_{CPT} \leftarrow \mathcal{L}_{CPT}(\mathbf{z})$ # self-supervised loss

$\nabla_{\mathcal{L}_{ce}^T} \leftarrow \partial \mathcal{L}_{ce} / \partial \theta_p, \nabla_{\mathcal{L}_{CPT}} \leftarrow \partial \mathcal{L}_{CPT} / \partial \theta_p$ # gradients w.r.t. prompts

if $T == 0$ **then**

$\tilde{\nabla}_{\mathcal{L}_{ce}} \leftarrow \nabla_{\mathcal{L}_{ce}^T}$

else

$\tilde{\nabla}_{\mathcal{L}_{ce}} \leftarrow \alpha \tilde{\nabla}_{\mathcal{L}_{ce}} + (1 - \alpha) \nabla_{\mathcal{L}_{ce}^T}$ # exponential moving average

end if

$\mathcal{L}_{GM} = 1 - \cos(\tilde{\nabla}_{\mathcal{L}_{ce}}, \nabla_{\mathcal{L}_{CPT}})$ # gradient matching loss

$\theta \leftarrow \theta - \epsilon (\nabla_{\mathcal{L}_{ce}^T} + \nabla_{\mathcal{L}_{CPT}} + \nabla_{\mathcal{L}_{GM}})$ # update model parameters

end for

Stage 2: Test-time adaptation

for $T = 1, 2, \dots$ **do**

$\mathbf{t} \leftarrow \mathcal{Y}^{(t)}, \mathbf{P}$ # combine class token with prompts

$\mathbf{z} \leftarrow h(g(\mathbf{t}))$ # compute text features

$\mathcal{L}_{CPT} \leftarrow \mathcal{L}_{CPT}(\mathbf{z})$ # self-supervised loss

$\theta_p \leftarrow \theta_p - \epsilon (\partial \mathcal{L}_{CPT} / \partial \theta_p)$ # update prompt parameters

end for

Stage 3: Make predictions

$\mathbf{t} \leftarrow \mathcal{Y}^{(t)}, \mathbf{P}$ # combine class token with prompts

$\mathbf{w} \leftarrow g(\mathbf{t})$ # pre-compute text features

for each $\mathcal{X}_i^{(t)} \sim \mathcal{X}^{(t)}$ **do**

$\mathbf{e} \leftarrow f(\mathcal{X}_i^{(t)})$ # compute image feature

$I_i \leftarrow \arg \max \mathbf{e} \cdot \mathbf{w}$ # directly make prediction

end for
